Functional and Molecular Characterization of PD1+ Tumor-Infiltrating Lymphocytes From Lung Cancer Patients

Jesse Lipp
Boehringer Ingelheim RCV GmbH & Co KG: Boehringer Ingelheim RCV GmbH und Co KG
Limei Wang
Bern University Hospital
Nathalie Harrer
Boehringer Ingelheim RCV GmbH & Co KG: Boehringer Ingelheim RCV GmbH und Co KG
Stefan Mueller
University of Bern: Universitat Bern
Sabina Berezowska
University of Bern: Universitat Bern
Patrick Dorn
Bern University Hospital
Thomas M Marti
Bern University Hospital
Gregor J Kocher
Bern University Hospital
Balazs Hegedues
University of Duisburg Essen - Campus Duisburg: Universitat Duisburg-Essen
Abdallah Souabni
Boehringer Ingelheim RCV GmbH & Co KG: Boehringer Ingelheim RCV GmbH und Co KG
Sebastian Carotta
Boehringer Ingelheim RCV GmbH & Co KG: Boehringer Ingelheim RCV GmbH und Co KG
Mark A Pearson
Boehringer Ingelheim RCV GmbH & Co KG: Boehringer Ingelheim RCV GmbH und Co KG
Wolfgang Sommergruber
Boehringer Ingelheim RCV GmbH & Co KG: Boehringer Ingelheim RCV GmbH und Co KG
Ralph A Schmid
Bern University Hospital
Sean RR Hall (srrhall@protonmail.com)
McGill University https://orcid.org/0000-0003-3561-7329

Research

Keywords: PD1, memory, TILs, ID3, GSK3β

Posted Date: January 25th, 2021

DOI: https://doi.org/10.21203/rs.3.rs-152467/v1

Version of Record: A version of this preprint was published at OncoImmunology on February 9th, 2022.
See the published version at https://doi.org/10.1080/2162402X.2021.2019466.

Abstract

Background The majority of infiltrating T-cells (TILs) in lung cancer are contained in the memory compartment and overexpress PD1 and have been associated with dysfunction. Antibody-mediated cancer immunotherapy targets inhibitory surface molecules, such as PD1, PD-L1, and CTLA-4, aiming to re-invigorate dysfunctional T cells.

Methods Using fluorescence-activated cell sorting (FACS), we purified CD45RO$^+$ memory CD8$^+$ and CD4$^+$ TILs and their patient-matched non-tumor counterparts from treatment-naïve NSCLC patient biopsies to better evaluate the effect of PD1 expression on the functional and molecular profile of tumor-resident T cells. Moreover, we compared the functional, molecular, and clonal composition of TIL preparations after TCR-dependent *in vitro* expansion with their freshly isolated counterparts in matched patients.

Results We show that PD1$^+$CD8$^+$ TILs have elevated expression of the transcriptional regulator ID3 and that the overall cytotoxic potential of CD8 T cells can be improved by knocking down ID3, defining it as a potential regulator of T cell effector function. PD1$^+$CD4$^+$ memory TILs remain functionally intact and despite overexpressing key transcriptional activators known to negatively regulate CD8 function such as TOX and TOX2, display transcriptional patterns consistent with both follicular helper and regulator function and robustly facilitate B cell activation and expansion in response to TCR-dependent stimulation. Furthermore, we show that expanding *ex vivo*-prepared TILs *in vitro* in a TCR-dependent manner broadly preserves their functionality with respect to tumor cell killing, expansion and activation of B cells, and TCR repertoire. Although purified PD1$^+$CD8$^+$ TILs generally maintain an exhausted phenotype upon expansion *in vitro*, transcriptional analysis reveals a downregulation of markers of T cell dysfunction, including the co-inhibitory molecules PD1 and CTLA-4 and the transcription factors ID3, TOX and TOX2, while genes involved in cell cycle and DNA repair are upregulated. We find reduced expression of WNT signaling components to be a hallmark of PD1$^+$CD8$^+$ exhausted T cells *in vivo* and *in vitro* and demonstrate that restoring WNT signaling, by pharmacological blockade of GSK3β, can improve effector function.

Conclusions These data unveil novel targets for tumor immunotherapy and have promising implications for development of a personalized adoptive TIL-based cell therapy for lung cancer.

Background

The immune checkpoint receptor programmed cell death 1 (PD1) marks clonally expanding, antigen-specific T cells[1]. In cancer, T cells are exposed to chronic antigen stimulation, causing CD8$^+$ tumor-infiltrating lymphocytes (TILs) to enter a state of dysfunction. This “exhausted” state is characterized by loss of cytotoxic effector functions and sustained surface expression of PD1 and other co-inhibitory receptors, such as CTLA-4, LAG3, and TIM3, as well as overexpression of transcription factors TOX and TOX2[2]. Immune checkpoint blockade (ICB) therapies employ antibodies that prevent engagement of PD1 with its cognate ligand programmed cell death ligand 1 (PDL1), thereby triggering expansion and

reactivation of exhausted tumor-reactive PD1^{hi} CD8^{+} TILs[3]. Despite their lack of cytotoxicity, the presence of PD1^{hi} CD8^{+} TILs predicts response to ICB and correlates with reduced tumor burden and increased overall survival in resectable non-small cell lung cancer (NSCLC).[4,5] However, the majority of patients with lung cancer treated with antibodies targeting PD1/PDL1 axis do not derive lasting clinical benefit from ICB.[6] Whether the lack of response to ICB is due to an inability to reinvigorate tumor-resident CD8^{+} T cells [7], a failure to recruit such naïve cells from the periphery, or both remains unclear [8]. A deeper understanding of the functional and transcriptional consequences of PD1 expression in tumor-derived CD8^{+} T cells is required to address this unresolved question.

Although rarely mentioned in the context of immunotherapy, CD4^{+} memory T cells play an essential yet complex part in the host defence against cancer[9], as they have been assigned both immune-activating and immune-suppressive roles. Compared to their CD8^{+} counterparts, we know much less about the gene expression programs, molecular features and function of CD4^{+} T cells in lung cancer patients. The multifaceted role of CD4^{+} T cells has important clinical implications when it comes to developing an adoptive TIL-based therapy using naturally occurring autologous TILs[10], as it is unclear whether the functional identity of CD4^{+} TILs, such as surface receptors, transcriptional program, and TCR repertoire are maintained following *in vitro* expansion.[11]

Here, we examine the effect of PD1 expression on the functional and transcriptional profiles of CD45RO^{+} memory CD8^{+} and CD4^{+} T cells obtained *ex vivo* from treatment naive NSCLC resected tissue and compare them with T cells derived from matched uninvolved normal lung tissue. While PD1^{+}CD8^{+} memory TILs show hallmark features of exhaustion, PD1^{+}CD4^{+} memory TILs are both highly proliferative and cytotoxic. Moreover, we demonstrate that PD1^{+}CD4^{+} memory TILs are poised to provide B cell support, despite sharing expression of several co-inhibitory receptors and a core set of transcription factors that are central regulators of exhaustion with PD1^{+}CD8^{+} memory TILs. Transcriptional analysis revealed that the transcriptional regulator ID3 is specifically upregulated in PD1^{+}CD8^{+} TILs and knockdown of ID3 improves tumor cell killing in wild type CD8^{+} T cells. We demonstrate that PD1^{+}CD8^{+} and PD1^{+}CD4^{+} memory TILs generated from *in vitro* expanded cultures exhibit generally similar functional patterns compared with their matched *ex vivo* counterparts but display some key transcriptional differences, such as downregulation of components of the WNT signaling pathway. Compensating the lack of WNT signaling through pharmacological inhibition of GSK3β improves the effector function of *in vitro* expanded populations.

Methods

See supplement for detailed Materials and methods. Collection of lung tumor samples Lung tumor tissues were collected from NSCLC patients undergoing operative procedures with a curative intent at Bern University Hospital, Division of General Thoracic Surgery. All patients provided informed written consent for use of their material for research purposes, which was approved by Ethics Commission of the

Canton of Bern (KEK-BE:2018-01801). Immediately following resection, tissue specimens were sent to the Institute of Pathology, University of Bern, where a pathologist dissected tumor and matched uninvolved lung tissue for further analysis. Tissue processing, flow cytometric analysis and cell sorting Single cell suspensions were generated from surgically resected tumor and matched uninvolved lung tissue, as previously described12. Single cells were stained in buffer containing Fc block (eBioscience, San Diego, CA, USA) and incubated with the following fluorescently conjugated human monoclonal antibodies: CD45, CD3, CD4, CD8, CD45RO, CD56, CD16, PD1, PDL1 (see Table S2). For fluorescence-activated cell sorting (FACS), cells were separated into PD1high or PD1low subsets following gating on CD45RO+ T cells for both CD8 and CD4 T cell compartment using either a MoFLo Astrios EQ 6way sorter (Beckman Coulter, Indianapolis, IN, USA)) or BD FACS Aria III (BD Biosciences, San Jose, CA, USA). Cells from tumor and matched uninvolved lung tissue were sorted directly into collection tubes containing 500 µl lysis buffer (4 M guanidinium thiocyanate, 30 mM Tris pH 8.0, 1% Triton-X-100) and processed for RNA isolation, as previously described13. Total RNA was treated with DNase I (Qiagen). RNA quantity was assessed on a ND-1000 spectrophotometer (NanoDrop Technologies, Thermo Scientific). Integrity of RNA (RIN > 8) was assessed with an Agilent 2100 Bioanalyzer (Agilent Technologies, Santa Clara, CA, USA).

Results

PD1 expression is associated with exhaustion in CD8 but not CD4 memory TILs

To functionally characterize T cell populations from NSCLC, we dissociated surgically resected tumor and FACS-sorted tumor infiltrating lymphocytes (TILs) and their matching counterparts from adjacent histologically uninvolved lung tissue (NILs) from 18 patients (8 adenocarcinoma, 10 squamous cell carcinoma). Following isolation of $CD45RO^+$ memory $CD4^+$ and $CD45RO^+$ memory $CD8^+$ memory T cells, we further stratified both cell types by expression level of PD1, resulting in four subpopulations ($PD1^+CD4^+$, $PD1^-CD4^+$, $PD1^+CD8^+$ and $PD1^-CD8^+$) for each patients tumor and matched normal sample (Figure 1A-B and Figure S1A). We found that memory $PD1^+$ T cells were more abundant in tumors than in uninvolved tissues (50% versus 31% in the CD4 and 45% versus 27% in the CD8 fraction), suggesting an activated and potentially exhausted phenotype of TILs (Figure 1C). In matched normal controls, $PD1^+CD4^+$ cells were less abundant than their $PD1^-CD4^+$ counterparts (31% versus 42%), while $PD1^+CD8^+$ and $PD1^-CD8^+$ cells were found with about equal frequency (27% versus 29%) (Figure 1C).

Next, we determined the effector potential of the T cell subpopulations by measuring their ability to expand *in vitro* and cytotoxic activity against lung cancer cell lines in a three-dimensional (3D) tumor spheroid assay[14] (Figure 1E). All four $CD4^+$ memory T cell subpopulations expanded well *in vitro* (Figure 1D) and effectively eliminated A549 lung adenocarcinoma cells, irrespective of their PD1 status and whether they originated from tumor or uninvolved tissue, indicating that their effector potential was intact (Figure 1F and Figure S1B,D). Conversely, amongst the CD8 subpopulations, only tumor-derived $PD1^+CD8^+$ memory TILs showed diminished growth capacity i*n vitro* (Figure 1D) and failed to kill A549 lung adenocarcinoma cells(Figure 1F and Figure S1C). In contrast, tumor killing capacity of $CD8^+$ T cells

from the peripheral blood of healthy donors was intact irrespective of PD1 status (Figure 1F and Figure S1D). Similar patterns of tumor cell killing capacity were also confirmed against H157 lung squamous cell carcinoma cells (Figure S1E-F). We conclude that high PD1 expression correlates with an exhausted phenotype in $CD8^+$TILs, but not $CD4^+$ TILs or $PD1^+$ $CD8^+$ or $PD1^+$ $CD4^+$ T cells derived from adjacent normal tissue.

Transcriptional characterization of NSCLC memory T cell populations

Gene expression patterns of T cell populations derived from tumor tissue and adjacent matched uninvolved lung from eight NSCLC patients was then assessed by RNA Seq. Two-dimensional projection of the transcriptomics data using T-distributed Stochastic Neighbor Embedding (t-SNE) demonstrated clear separation of CD4 and CD8 subpopulations into two distinct clusters (Figure 2A). Within those clusters, the projection distinguished samples from tumor and matched uninvolved tissue, indicating a strong effect of the microenvironment on both $CD4^+$ and $CD8^+$ memory T cells. The expression level of PD1 has a small, but visible influence on global gene expression, particularly in sorted TILs.

The difference between $CD4^+$ and $CD8^+$ memory T cells is also reflected in the number of differentially expressed genes. Although we determined 664 genes significantly up- or downregulated (FDR <= 0.05) in both CD4 and CD8 cells sorted from tumor tissue compared to matched normal tissue, we found a roughly equal number of CD4- and CD8-specific genes (727 and 821, respectively) (Figure S2B). Interestingly, high PD1 expression had a much more pronounced effect on the number of significantly changed genes in TILs compared to NILs from matched uninvolved tissue, in particular in $CD8^+$ T cells (820 tumor-specific genes, 74 shared, 33 normal-specific) (Figure S2C). We also noted a significant overlap of differentially expressed genes in $PD1^{hi}$ TILs between $CD8^+$ and $CD4^+$ T cells, compared to $PD1^{lo}$ (259 and 33 genes shared, respectively). PD1 expression is part of the T cell activation transcriptional program, thus it is conceivable that this observation relates to T cells encountering more antigen in the tumor but less so in matched uninvolved lung tissue.[15]

Gene set enrichment confirmed that downregulation of GPCR signaling is associated with tumor residence and high PD1 expression in $CD4^+$ and $CD8^+$ memory T cells, suggesting reduced T cell activation in chronically activated TILs (Figure 2B). CD4 and CD8 cells differed with respect to genes involved in cytokine receptor interaction, with CD4 TILs generally showing upregulation of such genes, while $CD8^+$ TILs, particularly $PD1^+$ cells, showing downregulation (Figure 2B and Figure S2A). A possible explanation is an increased number of helper or regulatory T cells within the $CD4^+$ TIL population.

To provide a concise overview of the gene expression patterns found in the different T cell populations, we curated lists of T cell co-stimulatory and co-inhibitory genes, transcription factors playing a part in T cell function, as well as genes involved in cell cycle, mitosis and DNA repair, and plotted their expression as a heatmap (Figure 2C). $PD1^+CD4^+$ and $PD1^+CD8^+$ memory TILs displayed high expression of known exhaustion-associated genes, CTLA4, ENTPD1 (CD39), CD200, LAG3, TIGIT, HAVCR2 (TIM3)[16], as well as

CD38, and LAYN [17]. In addition, $PD1^+CD4^+$ memory TILs showed elevated expression of PDCD1LG1 (CD274/PDL1) and PDCD1LG2 (CD273/PDL2), which negatively regulate T cell effector function by engaging with PD1[1]. Moreover, we observed upregulation of MAGEH1 and CCR8, two genes associated with CD4 regulatory T cell function in breast[18] and lung cancer patients[19]. Unlike $PD1^+CD4^+$ TILs, $PD1^+CD8^+$ memory TILs are characterized by downregulation of co-stimulatory molecules, including CD28, CD40LG, TNFSF8 (CD30LG) and memory-associated genes IL7R (CD127), SELL (CD62L) and LEF1 (Figure 2C). These changes coincided with downregulation of the memory precursor gene TCF7 (TCF-1). Furthermore, key transcription factors associated with T cell exhaustion, including TOX[20-22], TOX2[23], and ID3[24], were upregulated in $PD1^+CD8^+$ memory TILs, whereas RUNX3, which controls expression of cytotoxicity-related genes, was downregulated. Expression of cell cycle and DNA repair genes was generally elevated in both $PD1^+$ TILs, particularly in CD8 TILs (Figure 2C and Figure S2A). This finding is interesting considering the reduced ability of $PD1^+$CD8 TILs to expand *in vitro* (Figure 1D). Furthermore, WNT signaling was downregulated specifically in tumor-derived $PD1^+$ CD8 cells (Figure S2D). Overexpression of several canonical exhaustion-associated genes (TOX, TOX2, IRF4, CD200, CD38 and CTLA4) were shared between $PD1^+CD8^+$ and $PD1^+CD4^+$ memory TILs (Figure 2D). Additionally, we confirmed co-expression of multiple inhibitory receptors associated with chronic T cell activation and exhaustion at the protein level by flow cytometric analysis of $PD1^+CD8^+$ and $PD1^+CD4^+$ memory TILs (Figure S3A-B). We confirmed that a subset of $PD1^+CD8^+$ memory TILs that were enriched for CD38 and CD101 (Figure S3C), which were previously shown to be associated with a dysfunctional chromatin state in NSCLC[7], exhibited diminished proliferation (Figure S3D).

We obtained gene signatures corresponding to functional T cell clusters from a recent single cell sequencing analysis in NSCLC[17] and used them to determine the relative abundance of those clusters in our FACS sorted T cell populations with single sample gene set enrichment (ssGSEA). We found that in both $CD4^+$ and $CD8^+$ memory TILs, tumor residence and PD1 expression correlated with an exhausted state (C7-CXCL13 and C6-LAYN clusters, respectively) (Figure 2E and Figure S2E). Conversely, effector cell clusters (C3-CX3CR1 and C3-GNLY) showed a higher correlation in matched uninvolved lung tissue, compared with tumor, indicating an immunosuppressive tumor microenvironment. Naïve clusters tracked with both $PD1^-$ TILs in both CD4 and CD8 compartments. Notably, naïve regulatory T cells were most enriched in matched normal CD4 populations, while the suppressive regulatory T cell signature (C9-CTLA4) strongly correlated with tumor $PD1^+$ status in $CD4^+$ memory TILs (Figure 2E and Figure S2E).

Knock-down of ID3 in CD8 T cells increases their tumor killing capacity

Re-invigoration of exhausted T cells is a key goal of cancer immunotherapy, so we searched our gene expression data for candidates that could potentially regulate T cell exhaustion. Recent work has shown that the transcriptional regulator ID3 is enriched in dysfunctional TILs in human melanoma and NSCLC[24]. We found increased expression of ID3 in $CD4^+$ and $CD8^+$ TIL populations, compared to their matched controls (Figure 2C). Furthermore, ID3 expressing cells were most prominently represented in the

exhausted CD8 cluster (C6-LAYN) at the single cell level. Notably expression of ID3 in some cells in the naïve cluster (C1-LEF1) (Figure 3A), may reflect the described role of ID3 in T cell differentiation[25]. Conversely, the effector cluster (C3-CX3CR1) did not show any expression of ID3 (Figure 3B). To test if ID3 had a functional role in T cell exhaustion, we knocked-down ID3 in peripheral blood-derived CD8 T cells using siRNA and evaluated their capacity to kill A549 lung adenocarcinoma cells (Figure 1E). We found that reduction of ID3 mRNA levels led to significantly increased killing compared to scrambled siRNAs and no siRNA controls (Figure 3C-D). Similar results were obtained in Jurkat (a leukemic T cell line) following knockdown of ID3 (Figure S4A-B). We conclude that ID3 suppresses the effector potential of CD8 cells. Therefore, strategies aimed at decreasing ID3 expression in CD8 TILs could help to re-invigorate them from their exhausted state.

PD1^{+}CD4^{+} memory TILs facilitate B cell activation and expansion

Our transcriptional analysis suggested that PD1^{+}CD4 memory TILs displayed features of both helper and regulatory T cells (Figure 2C). Zappasodi et al.[26] recently identified a population of CD4 PD1^{+} cells (4PD-1^{Hi}) that were transcriptionally similar to T follicular helper (T_{FH})-like cells, but were functionally immunosuppressive and correlated with poor patient survival in NSCLC. Visual inspection of the expression of the signature genes showed enrichment in CD4^{+} memory TILs (Figure 4A) and ssGSEA analysis demonstrated a relative enrichment of the T follicular regulatory (T_{FR}) signature in the PD1^{+}CD4^{+} memory TIL population (Figure 4B). Many of the genes most enriched in PD1^{+}CD4^{+} memory TILs, such as CXCL13, CD200, TIGIT and SH2D1A, are also part of a T_{FH} cell gene signature[27] (Figure 4A). Moreover, PD1^{+}CD4^{+} memory TILs were enriched in other CD4 helper-related genes, TNFRSF18 (GITR), TNFRSF4 (OX40) and TOX2 [28]. Using ssGSEA, we found equally strong enrichment of the T_{FH} and the T_{FR} signatures in PD1^{+}CD4 TILs (Figure 4B).

Due to the challenges in differentiating T_{FR} from T_{FH} cells solely based on gene expression data, we utilized a more functional approach. Following *in situ* staining, PD1^{+}CD4^{+} TILs were observed in close proximity to CD19 positive B cells (Figure 4C and Figure S4C), suggesting functional interaction. FACS-purified PD1^{+}CD4 memory TILs, co-expressing the tumor-specific antigen receptor CD39[29], as well as CD25 (IL2RA) and CD200 exhibited robust expansion in culture (Figure S4D). *In vitro* expanded PD1^{+}CD4^{+} memory TILs were co-cultured with carboxyfluorescein succinimidyl ester (CFSE)-labeled CD19^{+} B cells, derived from dissected mediastinal lymph nodes of lung cancer patients and stimulated with the TCR activator staphylococcal enterotoxin B (SEB) (Figure S4E). As compared to B-cells alone, culture with activated CD4^{+} TILs induced B cell proliferation (38±13 versus 2.6±0.6%, respectively) (Figure 4D). Proliferating B cells were observed to downregulate expression of CD27 and upregulate CD38 (Figure 4E). This coincided with an upregulation of homing molecules CXCR5 and CCR7 (Figure 4F). Importantly, the majority of B cells did not upregulate CD24 (Figure 4G) or IL10 (Figure S4F), markers of B regulatory cells. Activated CD4^{+} TILs co-cultured with CD19 B cells re-express high levels of PD1 (Figure 4H), along with CD200, CD25 and CTLA4 (Figure 4I,J and Figure S4H,I) and showed an intact ability to degranulate,

based on increased expression of CD107a (Figure 4K). In addition, within the $PD1^+$ population, we observed an increase in the fraction of CD4 TILs co-expressing CXCR5 and CCR7, suggestive of an elevated potential to migrate to B cell zones (Figure 4L). Despite the fact that the sorted $PD1^+CD4^+$ memory TIL population likely represents a mixture of both T_{FH} and T_{FR} cells, we were able to show these cells are competent to engage B cells and thus functionally behave more like T_{FH} rather than T_{FR} cells.

Patient T cells expanded *in vitro* retain their cytotoxic and helper functions

Adoptive cell therapy (ACT) using autologous TILs expanded from patient tumors is a promising approach to treat solid tumors, including metastatic melanoma[30,31] and NSCLC[32]. Presently, it is unclear if and to what extent T cells change their phenotype under persistent TCR stimulation. To address this, we generated primary T cell cultures from resected tissue of NSCLC patients and expanded T cells via repetitive rounds of T cell receptor (TCR) ligation, using anti CD3/CD28/CD2 beads in the presence of the gamma chain (γ_c) cytokines IL-2, IL-7, and IL-15 (Figure 5A). T cells from single cell suspensions of uninvolved tissues proliferated more readily than their matched tumor counterparts ($38x10^6$±12.8 versus $26x10^6$±7 T cells, respectively) (Figure S5A). Bulk primary T cell cultures were then FACS sorted into populations, as previously described (Figure 1A). Compared with the native tumor, *in vitro* expansion altered the percentage of CD4 and CD8 subsets, with the extent and direction depending on the donor (Figure 5B). To quantify shifts in the composition within the CD4 and CD8 subpopulations, we performed transcriptomics analysis on each of the *in vitro* expanded subpopulation within the CD45RO memory compartment, calculated the enrichment of the T cell cluster signatures used previously (Figure 2E) and compared the *in vitro* patterns with the *ex vivo* prepared samples for which there were matching donors. Patterns of cell type composition were preserved well upon expansion *in vitro*, although the sharp distinctions between populations observed *in vivo* were less pronounced. Importantly, the dysfunctional clusters in both CD4 (C7-CXCL13) and CD8 (C6-LAYN) remain prominent in the $PD1^+$ TIL population (Figure 5D). The $PD1^+CD4^+$ memory TIL subset re-isolated from expanded bulk cultures retained their ability to help B cells (Figure S5F-H). To test the composition of the TCR clonotype between matched *ex vivo* prepared and *in vitro* expanded populations, we *in silico* re-constructed the TCR repertoire from samples with overlapping donors (four for CD4 and three for CD8 populations). Quantification of the overlap of TCR alpha (Figure S5E) and beta chains (Figure 5E) demonstrated that the donor-specific repertoire was stable *in vitro*.

Surprisingly we observed a general decrease of PD1 transcript levels in all *in vitro* expanded subpopulations following persistent TCR stimulation (Figure 5C), a finding that was confirmed at the protein level (Figure S5A-B). This trend towards a less “exhausted” gene expression profile was further exemplified by downregulation of the co-inhibitory molecules CD200, CD38, CD160, LAYN, and CTLA4 and concomitant upregulation of co-stimulatory molecules, such as IL2RA (CD25), TNFRSF4 (CD134) and CD40LG, in *in vitro* expanded $PD1^+CD8^+$ memory TILs (Figure 5C). We confirmed these changes for several additional cell surface molecules at the protein level within the TIL fraction (Figure S5C,D). Furthermore, all T cell populations downregulated the transcriptional regulators IRF8, TOX, TOX2, and ID3,

which are associated with an exhausted phenotype. $PD1^+CD8^+$ TILs upregulate memory/quiescence-associated genes (SELL, LEF1, CCR8) as well as cell cycle and DNA repair genes (PLK1, BRCA1) indicating a more proliferative phenotype. Both *in vitro* expanded $PD1^-$ and $PD1^+$ populations displayed robust killing ability (Figure 5F), indicating that *in vitro* expansion of $CD8^+$ memory TILs produces functionally intact cells.

Downregulation of components of the WNT pathway had already been observed in $PD1^+$ $CD8^+$ memory TILs *in vivo* (Figure S2D) and we observed a further downregulation of WNT1, WNT10A, and DKK3 upon *in vitro* expansion in all T cell populations (Figure 5C). As WNT signaling is known to arrest the development of effector $CD8^+$ T cells[33], we examined whether restoring WNT signaling via inhibition of GSK3β could further improve T cell function. We found that treating TILs during expansion with the GSK3 β inhibitor lithium chloride (LiCl) significantly increased the number of primary patient-derived primary lung tumor cells undergoing apoptosis, as judged by Annexin V staining, suggestive of enhanced TIL killing capacity (Figure 5G). Despite no difference in upregulation in PD1 (Figure S6D), activated TILs pretreated with LiCl displayed downregulation of Annexin V (Figure 5H). During the expansion period *in vitro* a reduction in the CD8 compartment occurred in the presence of LiCl (Figure S6A), despite this, when challenged with a pool of MHC Class I peptides both CD4 and CD8 TILs increased IFNγ secretion (Figure S6B) and upregulated expression of PD1 and CD80 (Figure S6C). We conclude that expansion of T cells *in vitro* could increase the number of autologous tumor-specific T cells for adoptive transfer and potentially also relieve some of the tumor-induced dysfunction, partially via restoring WNT signaling.

Discussion

Adoptive cell transfer of naturally occurring antigen-specific TILs has great potential as an antitumor therapy. Despite recent reports of clinical benefit in a number of solid tumors[34-36], important open questions remain, that include the extent of *in vivo* T cell persistence[37], the contribution of other cell types, such as $CD4^+$ cells[38], and whether the antitumor activity after PD1 checkpoint blockade originates from re-activation of exhausted TILs or migration of distinct clones from the periphery. In this report, we compare the phenotypic and transcriptomic profiles of resident memory CD8 and CD4 T cell populations prepared from NSCLC patient resections with their *in vitro* expanded counterparts. T cell expansion using chronic TCR stimulation resulted in highly heterogeneous expansion rates for different T cell subtypes, yet the expanded culture largely maintained their phenotypic and transcriptomic features, compared to the tissue-resident cells. Importantly, they retained their ability to efficiently kill tumor targets and promote B cell proliferation. Some important differences include downregulation of PD1 expression, both at the protein and mRNA level, in re-expanded $CD8^+$ and $CD4^+$ memory TILs compared with native tumor. In contrast, co-inhibitory receptors, TIM3 (HAVCR2) and LAG3, increased at the mRNA level, indicating at least a partial maintenance of an exhausted phenotype upon *in vitro* expansion, in line with previous data in ovarian cancer[34]. Furthermore, the stem-like gene TCF7 (TCF1), a T cell specific HMG-box containing transcription factor, remained downregulated in the *in vitro* expanded $PD1^+CD8^+$ memory compartment,

even in the presence of homeostatic γ_c cytokines IL-7/IL-15[39], coinciding with an overall decrease in WNT signaling[7,33], an indication of T cell dysfunction[40]. We show that restoring WNT signaling via a GSK3β inhibitor LiCl [41] may provide an important means to improve the functional capacity of *in vitro* expanded TILs for ACT. Lastly, the pool of re-expanded $CD8^+$ memory TILs downregulated TOX, TOX2 and KLRG1, while simultaneously upregulating CD27, CD28 and CD62L (SELL), arguing against formation of a terminal or short-lived effector state due to chronic TCR stimulation. The broad conservation of phenotype and functionality of expanded TILs is promising, although these results suggest that the success of ACT will be critically dependent on an understanding of the functional composition of the expanded culture and the careful selection of the appropriate T cell subpopulation.

Although $CD4^+$ memory T cell contribution is essential to coordinating host immunity against viral pathogens and chronic infection, the function of CD4 memory TILs in cancer control is less well studied, compared to their CD8 counterparts. The ability of $CD4^+$ T cells to substantially modulate anti-tumor activity is exemplified in a recent finding that high PD1 expression in $CD4^+$ TILs negatively correlates with patient survival in NSCLC [42]. Here, we show that the gene expression signature in $PD1^+CD4^+$ memory TILs highly correlate with a suppressor Treg signature [17], although when purified, at least a subset of $PD1^+CD4^+$ memory TILs are able to proliferate and effectively kill tumor cells. This argues that the $PD1^+CD4^+$ memory T cell compartment is a mixture of cell types, with potentially antagonistic functionality. Indeed, we show that $PD1^+CD4^+$ memory TILs are enriched in genes related to both T_{FH} [27] and T_{FR} cells [19]. One of the most upregulated genes in $PD1^+CD4^+$ memory TILs is the B lymphocyte chemoattractant CXCL13 [43], which, in conjunction with IL-21, triggers the enrichment of T_{FH} in germinal centers to coordinate B cell help. We demonstrate that activation of $PD1^+CD4^+$ memory TILs with the enterotoxin SEB induces mediastinal lymph node-derived B cells to proliferate and upregulate CXCR5, the receptor of CXCL13, while they themselves simultaneously re-express PD1, CD200, CD25 and CXCR5, known markers of T_{FH} cells. Importantly, proliferating B cells do not express CD24 or IL10, two common markers of regulatory B cells.

$PD1^+CD8^+$ TILs prepared from NSCLC patients display the major hallmarks of T cell dysfunction, a reduced proliferative potential and low tumor-killing activity. A key finding of our study, is that knockdown of ID3 in $CD8^+$ T cells or Jurkat cells results in enhanced effector function. At the mRNA level, ID3 is enriched in dysfunctional CD8 TILs in both melanoma and NSCLC[24]. In chronic lymphocytic choriomeningitis virus (LCMV) infection in mice, ID3 overexpression was linked with chronic TCR stimulation and correlated with $CD8^+$ T cell exhaustion[20]. ID3 is a member of the helix-loop-helix family of proteins that act as transcriptional regulators, preventing E proteins, e.g. E2A and HEB, from binding to DNA and repressing transcription. ID3 has been shown to be critical for the developmental progression of T cell differentiation[44] as well as formation of $CD8^+$ memory subsets[45,46]. The transcription factor TOX has recently emerged as a regulator of T cell exhaustion and as a potential target for immunotherapy[20-22]. TOX is thought to antagonize the function of E proteins through the upregulation of proteins of the ID

family, including ID3 [47]. Notably, scRNA-sequencing data of TILs in lung cancer patients also demonstrates that TOX is enriched in the exhausted CD8 T cell cluster [17]. Further, ablation of TOX in $CD8^+$ T cells partially restores function [21,22]. Taken together, ID3 and TOX may have functionally redundant roles in promoting a dysfunctional CD8 T cell phenotype resulting from chronic TCR stimulation, making them potential therapeutic targets for immune oncology. It should be noted that we found that many transcription factors acting as central regulators of T cell exhaustion (e.g. ID3, IRF4, TOX and TOX2) and other exhaustion-associated-genes, such as CD38, ENTPD1 or TIGIT overexpressed in $PD1^+CD8^+$ memory TILs, are also upregulated in $PD1^+CD4^+$ memory TILs. Recently it has been shown that ablation of TOX2 and TOX impairs T_{FH} cell differentiation [28] acting as a reminder that drug development efforts against such factors must consider that positive effects in one cell type may be mitigated by adverse effects in other cell types, as T_{FH} cells are central for a robust host anti-tumor immune response. The transcriptional regulator ID3 was also increased in CD4 TILs. ID3 appears to be necessary for maintenance of FoxP3 expression and CD4 Treg suppressive function [48]. Loss of ID3 leads to an increase in CD4 T_H9 phenotype that exhibit potent anti-tumor immunity[49]. Therefore, ID3 may be a more appropriate target for anti-tumor immunotherapy in lung cancer especially in the adoptive cell therapy setting.

Conclusions

Here, we show shared and distinct transcriptional profiles between CD4 and CD8 $PD\text{-}1^+$ memory TILs in NSCLC. Importantly, reducing ID3 expression improved CD8 T cell effector function. Therefore, depending upon the degree to which the original expression profiles observed in tissue-resident TILs are represented in the *in vitro* group following prolonged expansion in culture, future protocols may need to be modified to direct or redirect cellular differentiation to ensure enrichment of memory-precursor/stem-like T cells, which may correlate with persistence and improved clinical outcomes. Moreover, defining the optimal conditions for targeting WNT pathway to improve expanded autologous TIL product for ACT in NSCLC warrants further investigation.

Abbreviations

PD1, programmed cell death 1; TILs, Tumor-infiltrating lymphocytes; ICB; immune checkpoint blockade; PDL1; programmed cell death ligand 1; FACS, fluorescence-activated cell sorting; NILs, normal-infiltrating lymphocytes; 3D, three-dimensional; t-SNE; T distributed Stochastic Neighbour Embedding; ssGSEA, single sample gene set enrichment; T_{FH}; T follicular helper; T_{FR}, T follicular regulatory; CFSE; carboxyfluorescein succinimidyl ester; SEB, Staphylococcal enterotoxin B; ACT, Adoptive cell therapy; TCR, T cell Receptor; γ_c, gamma chain.

Declarations

Ethics approval and consent to participate

The protocol used for this study was approved by the Ethics Commission of the Canton of Bern (KEK-BE:2018-01801). All patients provided informed written consent for use of their material for research purposes. The cell line generation was performed in collaboration with the Westgerman Biobank Essen (WBE) and approved by the Ethics Committee of the University Duisburg-Essen (#18–8208-BO). All patients provided informed consent.

Consent for publication

All authors agreed on the manuscript**.**

Availability of data and material

The data that support the findings of this study are available within the paper and its Supplementary Information files. The RNA sequencing data have been deposited in the Gene Expression Omnibus (GEO) with the accession code GSExxxxxx. Any other material including the R code used for data analysis is available upon reasonable request to the authors (JL and SRRH).

Competing interests

The authors have no competing interests.

Funding: This work has been supported by the Innovative Medicines Initiative Joint undertaking under grant agreement n° 115188, resources of which are composed of financial contribution from the European Union's Seventh Framework Programme (FP7/2007-2013) and EFPIA companies in kind contribution.

Authors' contributions

conception & design – JL, WS, SRRH; tissue and data acquisition – JL, LW, NH, SM, SB, PD, TMM, GJK, BH, AS, WS, RAS, SRRH; Data interpretation & analysis – JL, LW, NH, SB, BH, AS, WS, SRRH; Drafting of Manuscript – JL, SRRH; Editing of manuscript – JL, LW, NH, SM, SB, PD, TMM, GJK, BH, AS, SC, MAP, WS, RAS, SRRH; Final Approval of manuscript – JL, WS, SRRH.

Acknowledgements: Tissue were provided by the Tissue Bank Bern. The lung cancer cell line PF139 was established in collaboration with the West-German Biobank Essen (WBE).

References

1. Sharpe AH, Pauken KE. The diverse functions of the PD1 inhibitory pathway. *Nat Rev Immunol.* 2018;18(3):153-167.
2. McLane LM, Abdel-Hakeem MS, Wherry EJ. CD8 T Cell Exhaustion During Chronic Viral Infection and Cancer. *Annu Rev Immunol.* 2019;37:457-495.

3. Kamphorst AO, Pillai RN, Yang S, et al. Proliferation of PD-1+ CD8 T cells in peripheral blood after PD-1-targeted therapy in lung cancer patients. *Proc Natl Acad Sci U S A.* 2017;114(19):4993-4998.
4. Rizvi NA, Hellmann MD, Snyder A, et al. Cancer immunology. Mutational landscape determines sensitivity to PD-1 blockade in non-small cell lung cancer. *Science.* 2015;348(6230):124-128.
5. Thommen DS, Koelzer VH, Herzig P, et al. A transcriptionally and functionally distinct PD-1(+) CD8(+) T cell pool with predictive potential in non-small-cell lung cancer treated with PD-1 blockade. *Nat Med.* 2018;24(7):994-1004.
6. Garon EB, Hellmann MD, Rizvi NA, et al. Five-Year Overall Survival for Patients With Advanced NonSmall-Cell Lung Cancer Treated With Pembrolizumab: Results From the Phase I KEYNOTE-001 Study. *J Clin Oncol.* 2019;37(28):2518-2527.
7. Philip M, Fairchild L, Sun L, et al. Chromatin states define tumour-specific T cell dysfunction and reprogramming. *Nature.* 2017;545(7655):452-456.
8. Wu TD, Madireddi S, de Almeida PE, et al. Peripheral T cell expansion predicts tumour infiltration and clinical response. *Nature.* 2020.
9. Borst J, Ahrends T, Babala N, Melief CJM, Kastenmuller W. CD4(+) T cell help in cancer immunology and immunotherapy. *Nat Rev Immunol.* 2018;18(10):635-647.
10. Creelan B, Teer J, Toloza E, et al. OA05.03 Safety and Clinical Activity of Adoptive Cell Transfer Using Tumor Infiltrating Lymphocytes (TIL) Combined with Nivolumab in NSCLC. *Journal of Thoracic Oncology.* 2018;13(10):S330-S331.
11. Utzschneider DT, Charmoy M, Chennupati V, et al. T Cell Factor 1-Expressing Memory-like CD8(+) T Cells Sustain the Immune Response to Chronic Viral Infections. *Immunity.* 2016;45(2):415-427.
12. Wang L, Dorn P, Zeinali S, et al. CD90(+)CD146(+) identifies a pulmonary mesenchymal cell subtype with both immune modulatory and perivascular-like function in postnatal human lung. *Am J Physiol Lung Cell Mol Physiol.* 2020;318(4):L813-L830.
13. Oberli A, Popovici V, Delorenzi M, et al. Expression profiling with RNA from formalin-fixed, paraffin-embedded material. *BMC Med Genomics.* 2008;1:9.
14. Osswald A, Hedrich V, Sommergruber W. 3D-3 Tumor Models in Drug Discovery for Analysis of Immune Cell Infiltration. *Methods Mol Biol.* 2019;1953:151-162.
15. Reuben A, Zhang J, Chiou SH, et al. Comprehensive T cell repertoire characterization of non-small cell lung cancer. *Nat Commun.* 2020;11(1):603.
16. Clarke J, Panwar B, Madrigal A, et al. Single-cell transcriptomic analysis of tissue-resident memory T cells in human lung cancer. *J Exp Med.* 2019;216(9):2128-2149.
17. Guo X, Zhang Y, Zheng L, et al. Global characterization of T cells in non-small-cell lung cancer by single-cell sequencing. *Nat Med.* 2018;24(7):978-985.
18. Wang L, Simons DL, Lu X, et al. Connecting blood and intratumoral Treg cell activity in predicting future relapse in breast cancer. *Nat Immunol.* 2019;20(9):1220-1230.

19. De Simone M, Arrigoni A, Rossetti G, et al. Transcriptional Landscape of Human Tissue Lymphocytes Unveils Uniqueness of Tumor-Infiltrating T Regulatory Cells. *Immunity.* 2016;45(5):1135-1147.
20. Alfei F, Kanev K, Hofmann M, et al. TOX reinforces the phenotype and longevity of exhausted T cells in chronic viral infection. *Nature.* 2019;571(7764):265-269.
21. Khan O, Giles JR, McDonald S, et al. TOX transcriptionally and epigenetically programs CD8(+) T cell exhaustion. *Nature.* 2019;571(7764):211-218.
22. Scott AC, Dundar F, Zumbo P, et al. TOX is a critical regulator of tumour-specific T cell differentiation. *Nature.* 2019;571(7764):270-274.
23. Seo H, Chen J, Gonzalez-Avalos E, et al. TOX and TOX2 transcription factors cooperate with NR4A transcription factors to impose CD8(+) T cell exhaustion. *Proc Natl Acad Sci U S A.* 2019;116(25):12410-12415.
24. Li H, van der Leun AM, Yofe I, et al. Dysfunctional CD8 T Cells Form a Proliferative, Dynamically Regulated Compartment within Human Melanoma. *Cell.* 2019;176(4):775-789 e718.
25. Omilusik KD, Shaw LA, Goldrath AW. Remembering one's ID/E-ntity: E/ID protein regulation of T cell memory. *Curr Opin Immunol.* 2013;25(5):660-666.
26. Zappasodi R, Budhu S, Hellmann MD, et al. Non-conventional Inhibitory CD4(+)Foxp3(-)PD-1(hi) T Cells as a Biomarker of Immune Checkpoint Blockade Activity. *Cancer cell.* 2018;33(6):1017-1032 e1017.
27. Gu-Trantien C, Loi S, Garaud S, et al. CD4(+) follicular helper T cell infiltration predicts breast cancer survival. *J Clin Invest.* 2013;123(7):2873-2892.
28. Xu W, Zhao X, Wang X, et al. The Transcription Factor Tox2 Drives T Follicular Helper Cell Development via Regulating Chromatin Accessibility. *Immunity.* 2019;51(5):826-839 e825.
29. Simoni Y, Becht E, Fehlings M, et al. Bystander CD8(+) T cells are abundant and phenotypically distinct in human tumour infiltrates. *Nature.* 2018;557(7706):575-579.
30. Dafni U, Michielin O, Lluesma SM, et al. Efficacy of adoptive therapy with tumor-infiltrating lymphocytes and recombinant interleukin-2 in advanced cutaneous melanoma: a systematic review and meta-analysis. *Ann Oncol.* 2019;30(12):1902-1913.
31. Nguyen LT, Saibil SD, Sotov V, et al. Phase II clinical trial of adoptive cell therapy for patients with metastatic melanoma with autologous tumor-infiltrating lymphocytes and low-dose interleukin-2. *Cancer Immunol Immunother.* 2019;68(5):773-785.
32. Federico L, Haymaker CL, Forget M-A, et al. A preclinical study of tumor-infiltrating lymphocytes in NSCLC. *Journal of Clinical Oncology.* 2018;36(5_suppl):161-161.
33. Gattinoni L, Zhong XS, Palmer DC, et al. Wnt signaling arrests effector T cell differentiation and generates CD8+ memory stem cells. *Nat Med.* 2009;15(7):808-813.
34. Owens GL, Price MJ, Cheadle EJ, Hawkins RE, Gilham DE, Edmondson RJ. Ex vivo expanded tumour-infiltrating lymphocytes from ovarian cancer patients release anti-tumour cytokines in response to autologous primary ovarian cancer cells. *Cancer Immunol Immunother.* 2018;67(10):1519-1531.

35. Rosenberg SA, Yang JC, Sherry RM, et al. Durable complete responses in heavily pretreated patients with metastatic melanoma using T-cell transfer immunotherapy. *Clin Cancer Res.* 2011;17(13):4550-4557.
36. Stevanovic S, Helman SR, Wunderlich JR, et al. A Phase II Study of Tumor-infiltrating Lymphocyte Therapy for Human Papillomavirus-associated Epithelial Cancers. *Clin Cancer Res.* 2019;25(5):1486-1493.
37. Lu YC, Jia L, Zheng Z, Tran E, Robbins PF, Rosenberg SA. Single-Cell Transcriptome Analysis Reveals Gene Signatures Associated with T-cell Persistence Following Adoptive Cell Therapy. *Cancer Immunol Res.* 2019;7(11):1824-1836.
38. Inderberg EM, Walchli S. Long-term surviving cancer patients as a source of therapeutic TCR. *Cancer Immunol Immunother.* 2020.
39. Cieri N, Camisa B, Cocchiarella F, et al. IL-7 and IL-15 instruct the generation of human memory stem T cells from naive precursors. *Blood.* 2013;121(4):573-584.
40. van Loosdregt J, Coffer PJ. The Role of WNT Signaling in Mature T Cells: T Cell Factor Is Coming Home. *J Immunol.* 2018;201(8):2193-2200.
41. Ohteki T, Parsons M, Zakarian A, et al. Negative regulation of T cell proliferation and interleukin 2 production by the serine threonine kinase GSK-3. *J Exp Med.* 2000;192(1):99-104.
42. Zappasodi R, Budhu S, Hellmann MD, et al. Non-conventional Inhibitory CD4(+)Foxp3(-)PD-1(hi) T Cells as a Biomarker of Immune Checkpoint Blockade Activity. *Cancer Cell.* 2018;34(4):691.
43. Shi J, Hou S, Fang Q, Liu X, Liu X, Qi H. PD-1 Controls Follicular T Helper Cell Positioning and Function. *Immunity.* 2018;49(2):264-274 e264.
44. Kee BL. E and ID proteins branch out. *Nat Rev Immunol.* 2009;9(3):175-184.
45. Ji Y, Pos Z, Rao M, et al. Repression of the DNA-binding inhibitor Id3 by Blimp-1 limits the formation of memory CD8+ T cells. *Nat Immunol.* 2011;12(12):1230-1237.
46. Yang CY, Best JA, Knell J, et al. The transcriptional regulators Id2 and Id3 control the formation of distinct memory CD8+ T cell subsets. *Nat Immunol.* 2011;12(12):1221-1229.
47. Xiong Y, Bosselut R. The enigma of CD4-lineage specification. *Eur J Immunol.* 2011;41(3):568-574.
48. Rauch KS, Hils M, Lupar E, et al. Id3 Maintains Foxp3 Expression in Regulatory T Cells by Controlling a Transcriptional Network of E47, Spi-B, and SOCS3. *Cell Rep.* 2016;17(11):2827-2836.
49. Nakatsukasa H, Zhang D, Maruyama T, et al. The DNA-binding inhibitor Id3 regulates IL-9 production in CD4(+) T cells. *Nat Immunol.* 2015;16(10):1077-1084.

Figures

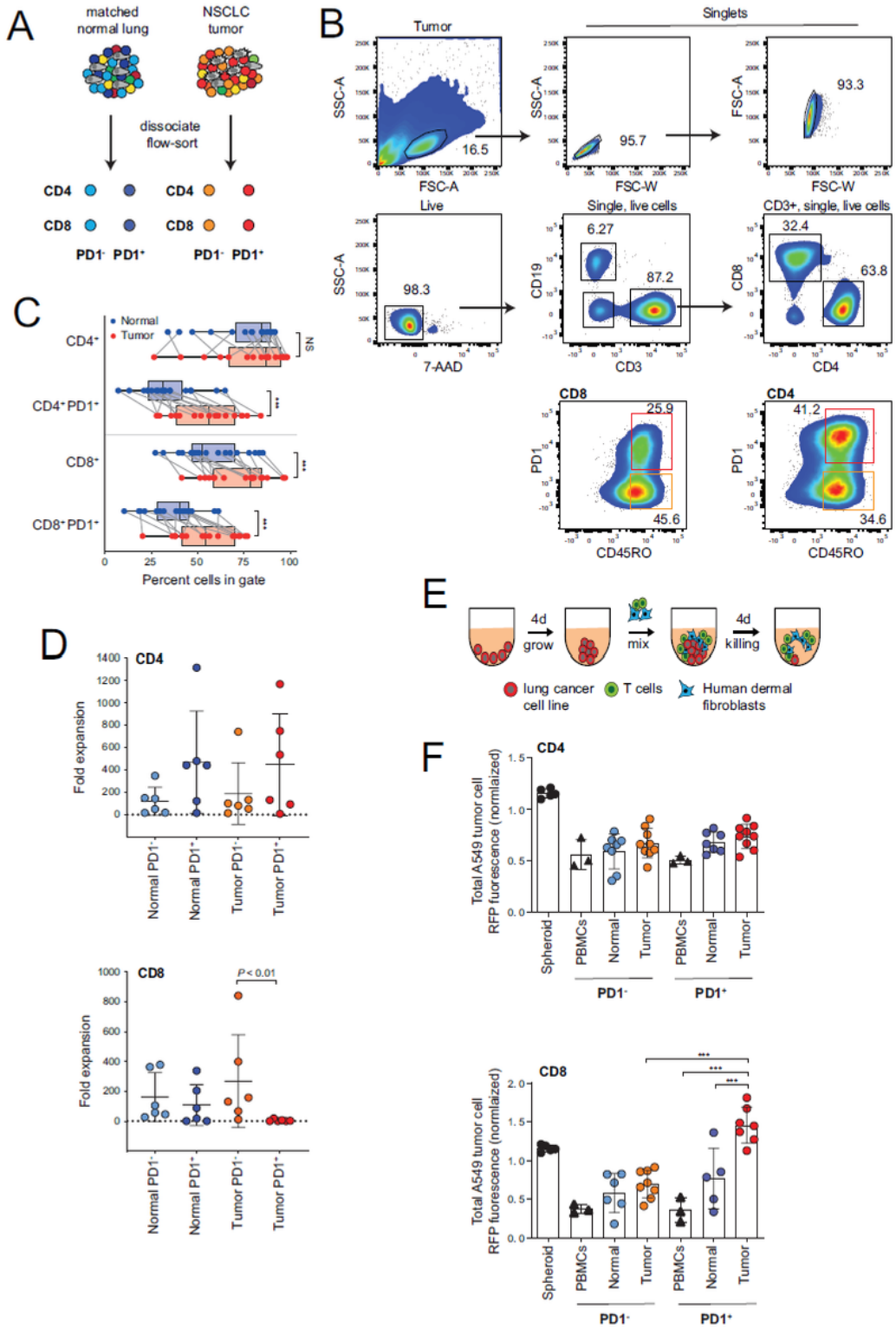

Figure 1

Functional characterization of CD4 and CD8 memory T cells based on PD1 expression in resectable NSCLC. A. Graphical overview of the four populations of T cells (TC) isolated for characterization from tumor and matched uninvolved normal lung tissue. B. Representative panels showing gating strategy to isolate CD45RO+ (memory) CD4 and CD8 T cells based on PD1 status from tumor and matched uninvolved lung tissue. C. Box and whisker plots showing breakdown of immune cell populations in

tumor compared with matched uninvolved lung tissue. Line represents the median. (n = 18, biological replicates). D. Panels showing cumulative growth curves of eight TC subsets from patient donors in CD4 (upper) and CD8 compartment (lower). (n = 6, biological replicates). E. Schematic illustration showing method to assess T cell reactivity. F. Histograms showing cell death of tumor spheroids generated from red fluorescent protein (RFP)-nuclear labelled A549 human lung adenocarcinoma cells co-cultured without or with the addition of various T cell subsets at a 1:1 effector-to-target ratio. Tumor cell killing was monitored in real time and analyzed as a loss of RFP intensity. (n = 6 biological replicates). Data are normalized to spheroids with no T cells. Data are displayed as mean±SD. Data in C by paired Students t-test, two-tailed. Data in D, F, by one-way ANOVA followed by post-hoc Newman-Keuls. **P < 0.01, ***P <0.001; ns, not significant.

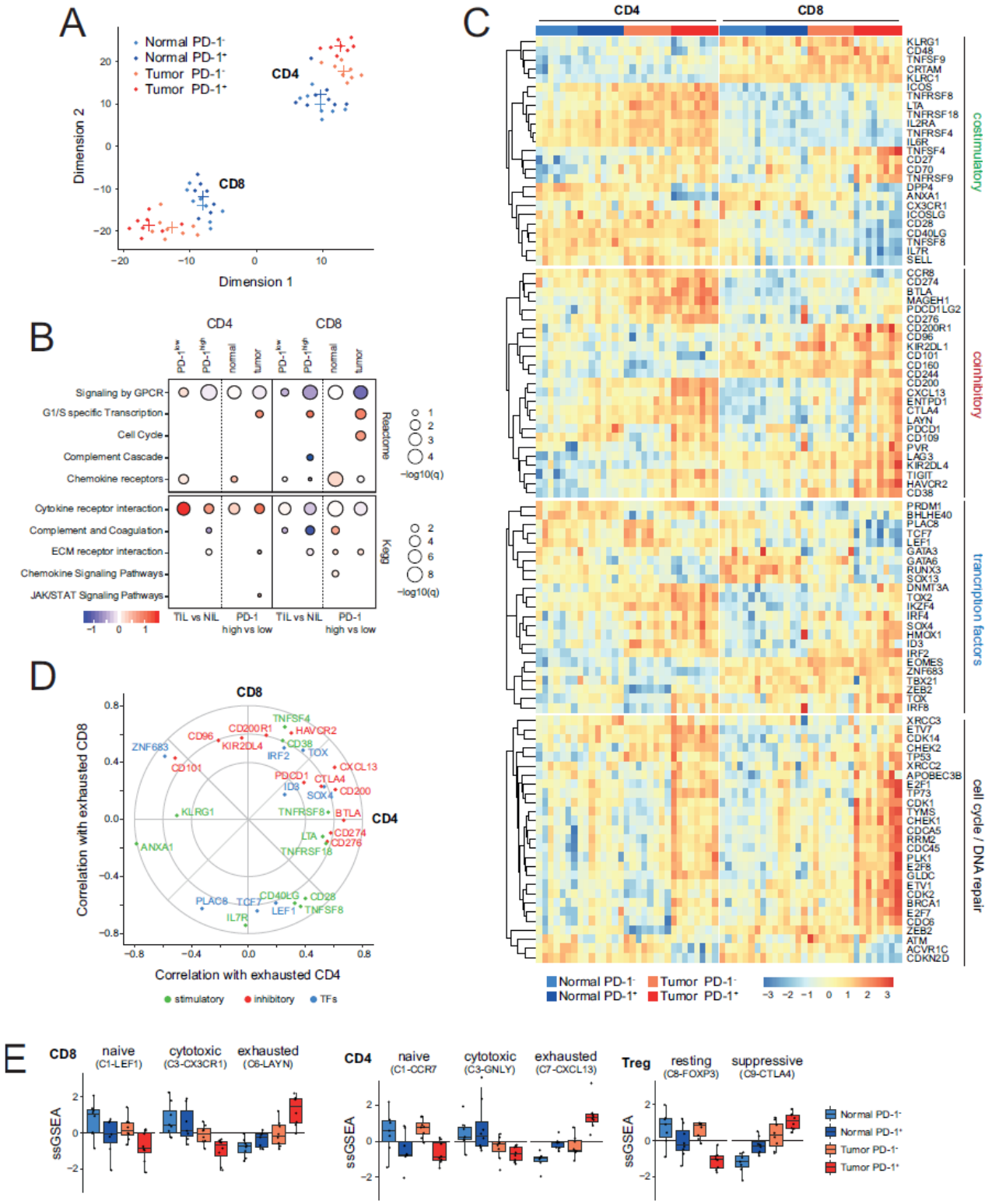

Figure 2

Transcriptional profile of sorted CD8 and CD4 memory T cells based on PD1 expression from matched patient samples in NSCLC. A. tSNE plot showing the separation of 8 cell subsets based on biological genotypes, cell type and PD1 expression. Each dot represents a patient (n = 8, biological replicates). B. Functional annotation of the differentially expressed genes via GSEA dot plot showing KEGG and Reactome pathway enrichment comparing biological genotypes (tumor versus normal), cell type (CD4

and CD8) and PD1 status (high vs low). C. Functional heatmap of differentially expressed candidate genes in memory T cells for the following modules (coinhibitory, stimulatory, transcription factors and cell cycle/DNA repair) separated based on biological genotypes, cell type and PD1 expression. Each bar represents one patient. D. Radar plot showing deregulated (up and down) gene programs in CD8 and CD4 TILs based on PD1 status that correlate with exhaustion based on single cell TIL data in NSCLC from Guo et al. 17. E. Cluster barplot showing the correlation of prospectively sorted cell fractions to single cell TIL clusters in NSCLC based on Guo et al 17. Each dot represents one patient.

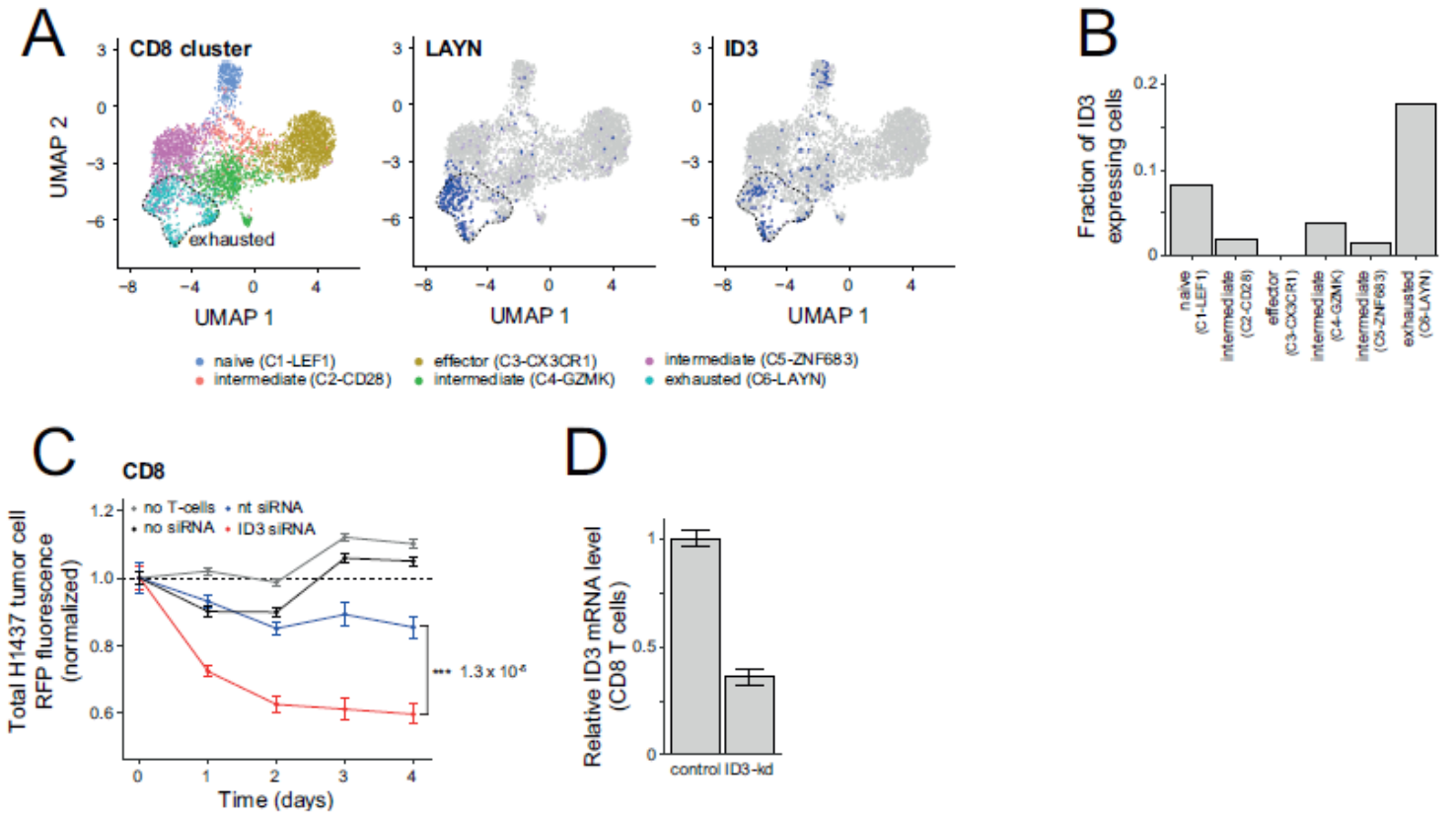

Figure 3

Downregulation of ID3 enhances effector function of CD8 T cells. A. Uniform Manifold Approximation and Projection (UMAP) panels showing projection of clusters of CD8 TILs marked by colour-code based on single cell data from NSCLC tumor lesions by Guo et al.17. Single cells are shown as dots. B. Bar graphs showing fraction of ID3 expressing cells enriched within the different single cell CD8 TIL clusters as shown in A. C. Line graphs showing the kinetics of tumor cell death quantified as a loss of red fluorescence protein (RFP) intensity following coculture with activated CD8+ T cells from blood of healthy donors. Total RFP were normalized to H1437 lung tumor cells cultured with no TILs at time = 0. D. Bar graphs showing knockdown of ID3 expression in CD8+ T cells derived from PBMCs of healthy donors. Data are displayed as mean±SD. Data in C, Data in D,

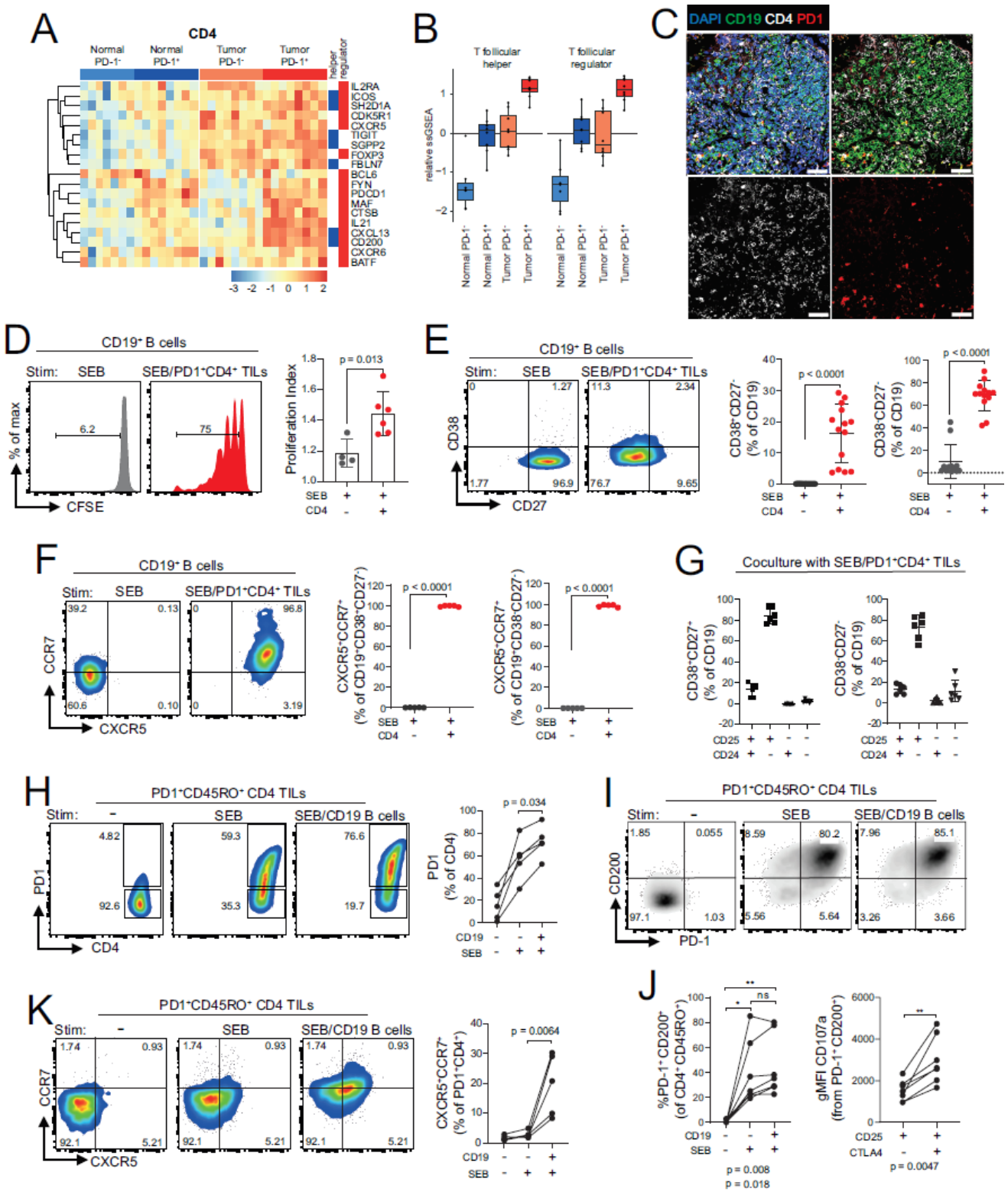

Figure 4

PD1+CD4+ memory TILs show features of TFH-like cells and are poised to help B cells. Heatmap with unsupervised clustering in A, and ssGSEA scores in B, showing enrichment of a 4PD-1hi TIL immunosuppressive signature based on a published dataset by Zappasodi et al. 42 and TFH gene signature by Gu-Trantien et al. 27 in CD4 TILs separated based on genotype (tumor versus normal) and PD1 status (PD1+ and PD1-). Each column in A represents a patient. C. Representative panels illustrating

localization of CD4/PD-1 in relation to CD19+ B cells (green) in tumor via confocal imaging. D. Histograms and proliferation index of carboxyfluorescein succinimidyl ester (CFSE)-labeled CD19+ B cells stimulated (Stim) with staphylococcal enterotoxin B (SEB, 500 ng/ml) alone or SEB cocultured with PD1+CD4 TILs. (n = 4-6, biological replicates). E. Histograms and frequency of CD38/CD27 subsets in CD19+ B cells after stimulation with SEB (500 ng/ml) alone or SEB in presence of PD1+CD4 TILs. (n = 13, biological replicates). F. Histograms and frequency of CXCR5+CCR7+ expression in stimulated CD19+ B cells. G. Frequencies of CD38/CD27 subsets for expression of CD24/CD25 stimulated with SEB in the presence of PD1+CD4 TILs. H. Histograms and change in P1 expression in CD4 TILs following stimulation with SEB alone or SEB in presence of CD19+ B cells. I. Histograms and frequencies of PD1+CD200+ cells as a % of CD4 TILs stimulated with SEB alone or SEB in the presence of CD4 TILs. (n = 6, biological replicates). J. gMFI of degranulation marker CD107a in PD1+CD200+ CD4 TILs co-expressing CD25 and CTLA4. (n = 6, biological replicates). K. Histogram and frequencies of CXCR5+CCR7+ CD4 TILs stimulated with SEB alone or SEB in the presence of CD19 B cells. Data are displayed as mean±SD. Data in D, E, F, and J by paired Students t-test, two-tailed. Data in H, I and K by one-way ANOVA followed by post-hoc Newman-Keuls. *P < 0.05, **P < 0.01, ***P <0.001, ****P <0.0001; ns, not significant.

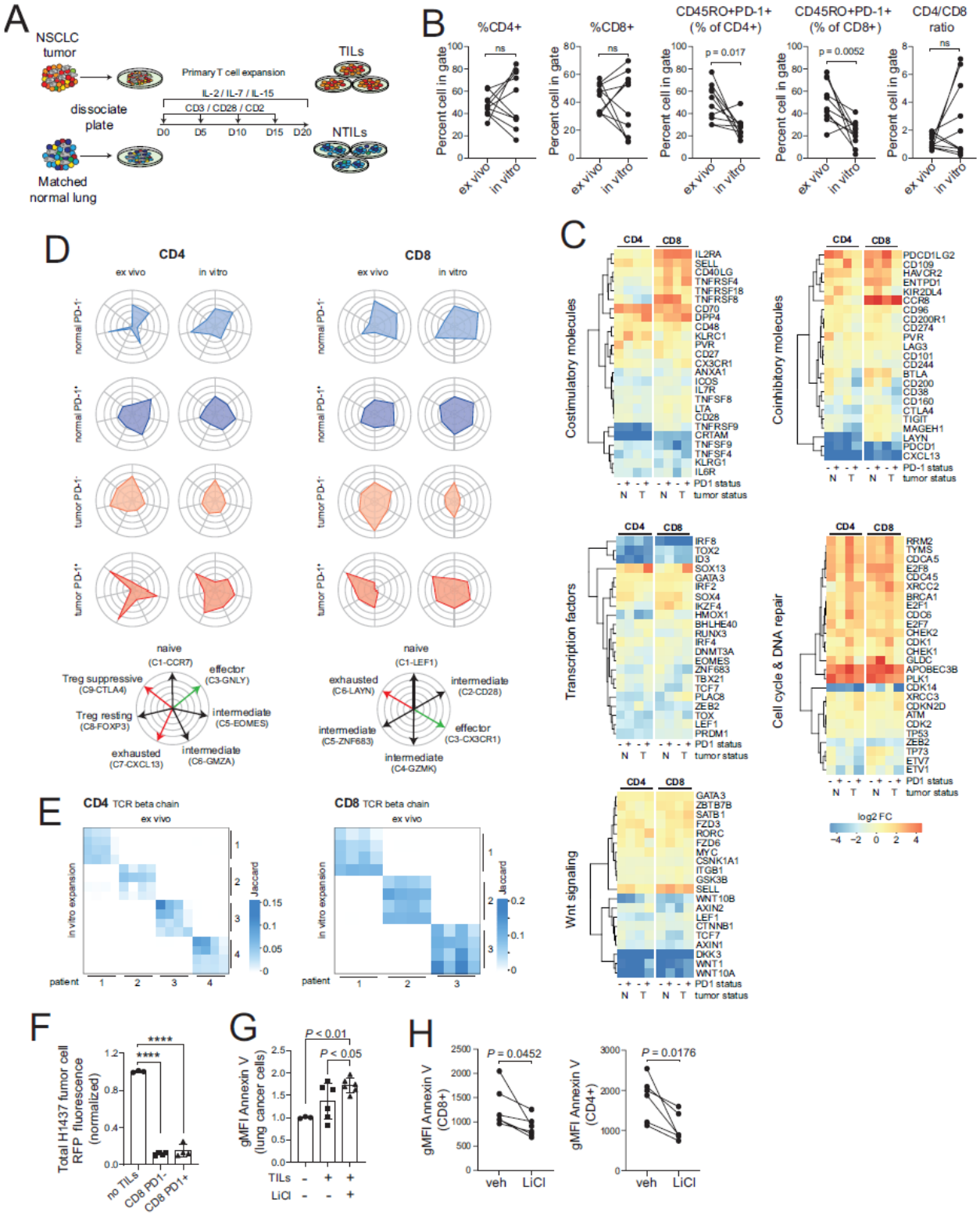

Figure 5

Transcriptional and functional analysis of memory T cells obtained after in vitro expansion from bulk tumor and matched normal specimens in NSCLC. A. Graphical overview showing method of the experimental design used to expand T cells from single cell suspensions. B. Scatter plots showing % change in CD4 and CD8 subsets, CD4/CD8 ratio and memory TILs based on PD1 expression for ex vivo (primary) compared with in vitro (culture expanded) TILs from matched patients. (n = 10, biological

replicates). C. Functional heatmaps showing relative gene expression levels of selected candidate genes in memory T cells for the following modules (stimulatory molecules, inhibitory molecules, transcription factors, cell cycle/DNA repair, Wnt signaling) comparing ex vivo and in vitro memory T cell subsets. Each column represents a matched patient. D. Cell type radar plots correlating expression profile of ex vivo and in vitro memory T cell subsets to single cell TC clusters described by Guo et al. 17. E. TCRβ repertoire analysis showing the degree to which clonal cells in both the CD4 and CD8 memory compartments between groups are maintained. Comparison between ex vivo and in vitro samples based on PD1 status. F. Histograms comparing tumor killing capacity of in vitro expanded CD8 TILs. Killing capacity measured as loss of RFP intensity. Total RFP normalized to H1437 lung tumor cells cultured with no TILs. (n = 4, biological replicates). G. Histograms comparing tumor killing capacity of in vitro expanded TILs quantified as the frequency of Annexin V expression in EpCAM+ primary lung cancer cells. Data were normalized to lung tumor cells cultured without TILs. (n = 6, biological replicates). H. Scatter plots showing change in Annexin V expression in CD4 (top) and CD8 (bottom) TILs in coculture with primary lung tumor cells without or with treatment LiCl (2mM). (n = 6 biological replicates). Data in B, G, by paired Students t-test, two-tailed. Data in F, G, by one-way ANOVA followed by post-hoc Newman-Keuls. ****P < 0.0001; ns, not significant.

Supplementary Files

This is a list of supplementary files associated with this preprint. Click to download.

- FigureS1.eps
- FigureS2.eps
- FigureS3.eps
- FigureS4.eps
- FigureS5.eps
- FigureS6.eps
- SupplementalMethodsTablesFigureLegendsReferences.docx